Preparation and high catalytic performance of Au/3DOM Mn_2O_3 for the oxidation of carbon monoxide and toluene

Shaohua Xie [a], Hongxing Dai [a,*], Jiguang Deng [a,*], Huanggen Yang [a], Wen Han [a], Hamidreza Arandiyan [b], Guangsheng Guo [a]

[a] Laboratory of Catalysis Chemistry and Nanoscience, Department of Chemistry and Chemical Engineering, College of Environmental and Energy Engineering, Beijing University of Technology, Beijing 100124, PR China
[b] Particles and Catalysis Research Group, School of Chemical Engineering, The University of New South Wales, Sydney, NSW 2052, Australia

GRAPHICAL ABSTRACT

xAu/3DOM Mn_2O_3 (x = 1.9−7.5 wt%) nanocatalysts are prepared via the PMMA-templating and PVA-protected reduction routes. The high oxygen adspecies concentration, good low-temperature reducibility, and strong interaction between Au and Mn_2O_3 are responsible for the high catalytic performance of 5.8Au/3DOM Mn_2O_3.
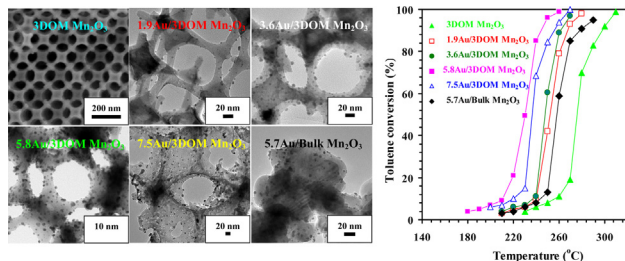
ARTICLE INFO

ABSTRACT

Three-dimensionally ordered macroporous (3DOM) Mn_2O_3 and its supported gold (xAu/3DOM Mn_2O_3, x = 1.9−7.5 wt%) nanocatalysts were prepared using the polymethyl methacrylate-templating and polyvinyl alcohol-protected reduction methods, respectively. The 3DOM Mn_2O_3 and xAu/3DOM Mn_2O_3 samples exhibited a surface area of 34−38 m^2/g. The Au nanoparticles (NPs) with a size of 3.0−3.5 nm were uniformly dispersed on the skeletons of 3DOM Mn_2O_3. The 5.8Au/3DOM Mn_2O_3 sample performed the best, giving the $T_{90\%}$ (the temperature required for a conversion of 90%) of −15 °C at space velocity (SV) = 20,000 mL/(g h) for CO oxidation and 244 °C at SV = 40,000 mL/(g h) for toluene oxidation. The apparent activation energies (30 and 54 kJ/mol) over 5.8Au/3DOM Mn_2O_3 were much lower than those (80 and 95 kJ/mol) over 3DOM Mn_2O_3 for CO and toluene oxidation, respectively. The effects of SV, water vapor, CO_2, and SO_2 on catalytic activity were also examined. It is concluded that the excellent catalytic performance of 5.8Au/3DOM Mn_2O_3 was associated with its high oxygen adspecies concentration, good low-temperature reducibility, and strong interaction between Au NPs and 3DOM Mn_2O_3 as well as high-quality porous architecture.

© 2014 Elsevier B.V. All rights reserved.

1. Introduction

Carbon monoxide and most of volatile organic compounds (VOCs) emitted from industrial and transportation activities are harmful to the environment and human health. Catalytic oxidation

is generally regarded as one of the most effective and economic pathways for the oxidative removal of CO and VOCs [1–3]. The key issue of such a technology is the development of high-performance catalytic materials, in which supported noble metals and transition-metal oxides are the most commonly used catalysts [2–5].

Gold nanoparticles (NPs) are active for the oxidation of CO and VOCs [5–7]. Since Haruta's discovery [5], reports on the oxidation of toluene, propene, and soot, and the reduction of NO_x [6–9] over supported gold NPs have increased dramatically. It is known that performance of a supported gold catalyst is heavily affected by the Au particle size, pretreated condition, preparation method, and support nature. For the transition-metal oxide-supported gold catalysts, the interaction between Au NPs and transition-metal oxide can result in reactive sites at the gold−oxide interface and/or generation of oxygen vacancies which is beneficial for formation of active oxygen species. These reactive sites and oxygen vacancies could enhance performance of the supported catalysts [6–11]. Therefore, the choice of an appropriate support is of significance in improving activity of a catalyst for CO and VOC oxidation.

In the past years, a large number of manganese oxides (MnO_x) with different morphologies (e.g., tubes, nanorods, nanowires, and flowers) and porous structures [12–16] have been fabricated. It is found that the physicochemical property of MnO_x strongly depends on its morphology, crystal size, and porous structure. Due to the low cost and environmentally friendly feature, MnO_x has been used as catalyst for removal of CO and VOCs [17–23]. For example, Tang et al. [20] observed a 100% conversion of formaldehyde over MnO_x nanorods at 180 °C and 24,000 h^{-1}. Baldi et al. [21] found that acetone could be completely oxidized at 270 °C over Mn_3O_4. Yu et al. [22] observed a total conversion of CO below 50 °C over MnO_2. Kim and Shim [18] obtained a catalytic performance order of $Mn_3O_4 > \alpha$-$Mn_2O_3 > \beta$-MnO_2 for benzene and toluene combustion. Ren et al. [23] pointed out that ordered mesoporous Mn_2O_3 exhibited high catalytic performance for CO oxidation. The loading of Au on MnO_x could greatly enhance catalytic activity for CO and VOC oxidation [24,10,25,26]. For example, Wang et al. [24,10] and Bastosa et al. [25] claimed that Au/Mn_2O_3, Au/MnO_2, and Au/Mn_3O_4 could effectively catalyze the oxidation of CO. Sinha et al. [26] observed good catalytic performance of Au/γ-MnO_2 for the oxidation of toluene, acetaldehyde, and hexane.

In recent years, fabrication of three-dimensionally ordered macroporous (3DOM) materials has been one of hot topics. As a catalyst or support [27], a 3DOM material exhibits good mass transfer property due to its interconnected pore architecture. With polystyrene microspheres as template and acetates or oxalates of metals as precursor, Stein and co-workers [28] fabricated 3DOM-structured Fe_2O_3, Cr_2O_3, Mn_2O_3, and Co_3O_4 with a pore size of 380−550 nm and a surface area of 20−39 m^2/g. Using differently sized polymethyl methacrylate (PMMA) microspheres as template and metal nitrates as precursor, Sadakane et al. [29] synthesized 3DOM-structured Fe_2O_3, Cr_2O_3, Mn_2O_3, Mn_3O_4, and Co_3O_4 with a pore diameter of 170−180 nm and a surface area of 13−57 m^2/g. To the best of our knowledge, however, there have been no reports on the use of 3DOM Mn_2O_3-supported Au NPs as catalyst for the oxidation of CO and VOCs.

Previously, our group adopted the PMMA-templating and/or polyvinyl alcohol (PVA)-protected reduction strategies to generate a number of 3DOM-structured materials, such as 3DOM Al_2O_3 and $Ce_{1−x}Zr_xO_2$ [30], 3DOM $La_{1−x}Sr_xMO_3$ (M = Mn, Fe, $Fe_{0.8}Bi_{0.2}$) [31,32], $MO_y/3DOM La_{1−x}Sr_xMO_3$ (M = Mn, Co) [33,34], and Au/3DOM $La_{1−x}Sr_xMO_3$ (M = Mn, Co) [7,35]. We observed that the 3DOM-structured perovskite-type oxide-based materials showed excellent performance in catalyzing the oxidation of CO and/or VOCs. As an extension work, we herein report the preparation, characterization, and catalytic activities of 3DOM

Mn_2O_3 and xAu/3DOM Mn_2O_3 (x = 1.9, 3.6, 5.8, and 7.5 wt%) for CO and toluene oxidation.

2. Experimental

2.1. Catalyst preparation

Well-arrayed PMMA microspheres with an average diameter of ca. 300 nm were synthesized according to the procedures described elsewhere [27]. 3DOM Mn_2O_3 was fabricated via the PMMA-templating route. The 3DOM Mn_2O_3-supported gold (xAu/3DOM Mn_2O_3) samples were prepared via a PVA-protected reduction route with PVA as protecting agent and $NaBH_4$ as reducing agent. For comparison, the Bulk Mn_2O_3 and 5.7Au/Bulk Mn_2O_3 samples were also prepared via the thermal decomposition of manganese nitrate at 500 °C for 10 h and the PVA-protected reduction route, respectively. The detailed preparation procedures are described in the Supplementary material.

2.2. Catalyst characterization

Physicochemical properties of the 3DOM Mn_2O_3, xAu/3DOM Mn_2O_3, and 5.7Au/Bulk Mn_2O_3 samples were characterized by means of techniques, such as inductively coupled plasma atomic emission spectroscopy (ICP-AES), X-ray diffraction (XRD), N_2 adsorption–desorption (BET), scanning electron microscopy (SEM), transmission electron microscopy (TEM), selected-area electron diffraction (SAED), X-ray photoelectron spectroscopy (XPS), and hydrogen temperature-programmed reduction (H_2-TPR). The detailed characterization procedures are stated in the Supplementary material.

2.3. Catalytic evaluation

Catalytic activities of the samples were evaluated in a continuous flow fixed-bed quartz microreactor. The reactant feed was 1.0 vol% CO + 20% O_2 + N_2 (balance) and the space velocity (SV) was ca. 20,000 mL/(g h) for CO oxidation, whereas the reactant mixture was 1000 ppm toluene + O_2 + N_2 (balance) and the SV was ca. 40,000 mL/(g h) for toluene oxidation. The detailed evaluation procedures are described in the Supplementary material.

3. Results

3.1. Crystal structure and textural property

Fig. 1 shows the XRD patterns of the xAu/3DOM Mn_2O_3 samples after calcination in an air flow at 500 °C for 10 h. The crystal structures of the samples could be indexed to the cubic Mn_2O_3 phase (JCPDS PDF# 41-1442). No other phases such as Mn_3O_4 and MnO appeared. That is to say, there was no disproportionation of Mn_2O_3. The grain sizes of Mn_2O_3 in the samples were calculated according to the Scherrer equation, as shown in Table 1. The crystallite sizes of Mn_2O_3 in 3DOM Mn_2O_3 and xAu/3DOM Mn_2O_3 were 44−52 nm, whereas that in 5.7Au/Bulk Mn_2O_3 was 87 nm. The weak Au (1 1 1) diffraction peak at 2θ = 38.5° was covered by the Mn_2O_3 (4 0 0) diffraction peak.

Fig. 2 shows the SEM images of the typical samples. There were a number of 3DOM entities in xAu/3DOM Mn_2O_3. Due to the difficulty in keeping the same preparation conditions (PMMA alignment, precursor solution impregnation, and filtering, drying, and calcination) of the samples, there was a change in macropore size. The average macropore sizes of the samples were in the range of 170−200 nm (Table 1). The 5.7Au/Bulk Mn_2O_3 sample contained irregularly morphological nano/macroparticles. The